Acta Biotheoretica 36: 249–273 (1987)

DISCRETE AND CONTINUOUS MODELS FOR HETEROCYST DIFFERENTIATION IN GROWING FILAMENTS OF BLUE-GREEN BACTERIA

CHRIS G. DE KOSTER and ARISTID LINDENMAYER

Vakgroep Theoretische Biologie, Rijksuniversiteit Utrecht, Padualaan 8, 3508 TB Utrecht, Netherlands

(Received 15-II-1988)

ABSTRACT

Heterocyst spacing in blue-green bacteria is widely assumed to be due to a diffusible inhibitor. The inhibitor, a nitrogen-rich compound, probably glutamine, is produced via the N_2-fixing enzymes of the heterocyst and in turn serves to suppress the induction of these enzymes and of the differentiation of vegetative cells to heterocysts. This simple morphogenetic mechanism operating in growing cellular filaments of *Anabaena* species is investigated on the basis of a continuous and a discrete cellular model, as well as by cell-by-cell simulation of the inhibitor transport. The resulting distances between heterocysts and kinetics of their production are compared with observations, and the values of physical parameters are estimated from the models.

1. INTRODUCTION

The regular distribution pattern of heterocysts in filaments of *Anabaena* and other blue-green bacteria has been the subject of many experimental and theoretical investigations (recently reviewed by Both et al., 1984). This pattern is characterized by a well-defined average number of vegetative cells separating the heterocysts (e.g. in *Anabaena catenula* the average distance is 10 cells, cf. Mitchison et al., 1976).

The development of such a pattern in these prokaryonts may be regulated by mechanisms which are basic to the morphogenetic processes of higher organisms. Furthermore, there are

indications that the underlying mechanism in blue-green bacteria is based on the transport of small molecules from cell to cell, a process which can be easily described in physico-chemical terms and which lends itself to possible measurements and experiments. A time sequence of heterocyst development is shown in Figure 1.

Since the heterocysts are known to possess N_2-fixing enzymes while the vegetative cells of the filament do not, it has been assumed for a long time that the movement of nitrogeneous compounds from heterocysts to vegetative cells is responsible for the regulation of heterocyst distances.

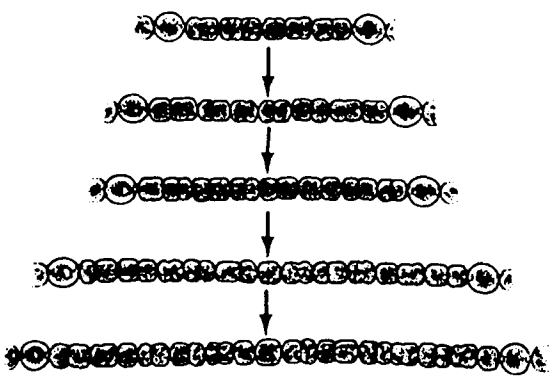

Figure 1. Heterocyst development in *Anabaena catenula* drawn after photographs of a filament by Mitchison & Wilcox (1972). The filament was photographed at 9, 6, 10, 15, and 21 hrs. Magnification is 800x. The arrows point from a smaller sister cell in the second row to stages of proheterocysts in the subsequent rows.

Fogg (1949) already referred to gradients of nitrogeneous substances. Wolk et al. (1976) suggested that glutamine is involved and Thomas et al. (1977) provided experimental evidence for the movement of glutamine from heterocysts to vegetative cells. It is also known that glutamine is produced in heterocysts from NH_4^+ and glutamate, which in turn comes very likely from glucose supplied by vegetative cells. But there is no general agreement on glutamine having a primary role in the induction of heterocysts. It is possible that another compound (e.g. thioredoxin) is responsible (Bothe et al., 1984). In any case it has been convincingly demonstrated by Wolk (1967) and Wilcox et al. (1973) that heterocysts are needed to regulate the differentiation of vegetative cells, and furthermore by Reddy & Talpasayi (1974) and Wolk & Quine (1975) that this regulation is not due to the destruction, by heterocysts, of an inducer produced by vegetative cells. The question remains whether a low level of glutamine or a low N/C ratio in a vegetative cell initiates the differentiation of the cell into a heterocyst.

Why should a low concentration of glutamine or one of its derivatives result in the derepression of genes for the morphogenesis of heterocysts? It has been suggested that the genes controlling N_2-fixation and the heterocyst morphogenesis are linked in a single operon (Singh et al., 1973) and that the transcription of this operon is induced by glutamine synthetase (Streicher et al., 1974) although the latter evidence does not come from work on blue-green bacteria.

Only vegetative cells can divide. At each division, two daughter cells are produced which are unequal in size. The cell cycle lengths are different, in *A. cylindrica* the proportion of cycle lengths of small to large sister cells is about 4 to 5 (Mitchison & Wilcox, 1972). Heterocysts arise only from small sister cells presumably when the concentration of an inhibitor (glutamine or another nitrogen compound produced in the heterocysts) falls below a threshold value. This compound is assumed to be transported, actively or passively, from cell to cell along the filament and consequently a

concentration gradient arises on either side of a heterocyst. As the distance between two existing heterocysts increases as a result of cell divisions, in the region between them a concentration minimum becomes lower than the threshold and the differentiation of a new heterocyst begins.

The simplest assumption for the transport process is that it takes place by diffusion according to Fick's law. This assumption has been compared with other possible mechanisms (such as an undamped domino effect) by Wolk & Quine (1975) and has been found to be the most likely one.

A morphogenetic mechanism for these organisms has been modelled on the basis of a simple diffusion process in a homogeneous medium contained in a cylinder (Wilcox et al., 1973). If the cylinder is not expanding in length, then an analytical solution can be found for the concentration as function of position and time of the inhibitor. For an expanding cylinder one has to use numerical methods. The basic weakness of this approach is that it is difficult to bring it into direct connection with the underlying molecular mechanism, namely with the derepression of genes in certain cells. A model based on diffusion taking place between discrete cells appears therefore preferable to us.

In this paper we investigate and compare both formulations of the problem, and carry out a computer simulation of this morphogenetic process with the help of a cellular array generating program. While in this work the concentration of only a single compound is calculated by the continuous and discrete models, it is possible to extend our method to a number of different compounds present in each cell as it becomes necessary by further biochemical data on the molecular basis of heterocyst induction (Golden et al., 1985).

2. THE CONTINUOUS MODEL

We assume that the inhibitor is present at a constant concentration in the heterocysts (c_h). The kinetics of the inhibitor movement in the filament is assumed to be a

diffusion process with the modified Fick's law as the basic equation:

$$\frac{\partial c(x,t)}{\partial t} = D \frac{\partial^2 c(x,t)}{\partial x^2} - k.c(x,t)$$

The last term in this equation is a linear decay term. The decay of the inhibitor corresponds to the metabolic degradation of glutamine as the major nitrogen source in vegetative cells. In this model the diffusion constant is construed as an average value for diffusion taking place partly through cell walls and partly through the cytoplasm.

In addition, this pattern generating process depends also on the cycle lengths of vegetative cells. We assume a Gaussian distribution of cycle lengths with a given average value and standard deviation.

We consider first the steady state situation for the inhibitor concentration between two heterocysts.

A steady state can occur only temporarily while the distance between heterocysts remains constant, i.e., while no cell divisions are taking place in this region. Thus a prerequisite of the occurrence of a steady state is that diffusion is fast with respect to the growth of the filament.

In steady state

$$\frac{\partial c(x,t)}{\partial t} = 0, \text{ and therefore } D \frac{\partial^2 c(x,t)}{\partial x^2} - k.c(x,t) = 0 \qquad (1)$$

This differential equation is independent of time and can be solved as follows. Assume that

$$e(x) = e^{\lambda x} \qquad (2)$$

is a solution. Then by substitution into (1) we obtain

$$D.\lambda^2 \,.\, e^{\lambda x} - k.e^{\lambda x} = 0 \qquad (3)$$

$$e^{\lambda x} (D\lambda^2 - k) = 0 \qquad (4)$$

The roots of (4) are

$$\lambda_1 = \sqrt{\frac{k}{D}} \quad \text{and} \quad \lambda_2 = -\sqrt{\frac{k}{D}}$$

The general solution of (2) is a linear combination of $c(x) = e^{\lambda_1 x}$ and $c(x) = e^{\lambda_2 x}$, namely

$$c(x) = R.e^{\sqrt{k/D}.x} + S.e^{-\sqrt{k/D}.x} \qquad (5)$$

The variable x stands for the value of the distance between points, and is measured in metric units.

One of the constraints is that the concentration curve between two identical sources should be symmetric around a certain x value: $c(x+a) = c(x-a)$. We assign the value x=0 to the point around which the steady state curve is symmetric. This yields that R=S, from which we obtain

$$c(x) = R(e^{\sqrt{k/D}.x} + e^{-\sqrt{k/D}.x}) \qquad (6)$$

Define the concentration at x=0 as c_0. Then $R = c_0/2$ and

$$c(x) = \tfrac{1}{2}\, c_0(e^{\sqrt{k/D}.x} + e^{-\sqrt{k/D}.x}) \qquad (7)$$

We see that c(x) is the sum of two functions:

$$c_1(x) = \tfrac{1}{2}\, c_0.e^{\sqrt{k/D}.x} \quad \text{and} \quad c_2(x) = \tfrac{1}{2}\, c_0 e^{-\sqrt{k/D}.x}.$$

This is shown in Figure 2.

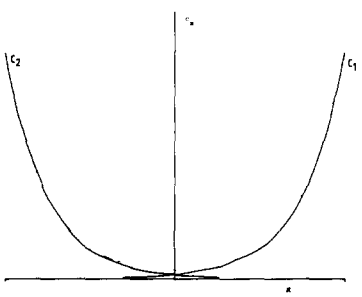

Figure 2. Concentration curves c_1 and c_2 as calculated on the basis of the continuous model.

If x is negative and large enough then $e^{\sqrt{k/D}.x}$ can be neglected with respect to $e^{-\sqrt{k/D}.x}$, and vice versa. By changing the coordinate system in such a way that x=0 at a heterocyst, where the concentration of the inhibitor is c_h, we obtain the solution of (6) for x>0 as

$$c(x) = c_h.e^{-\sqrt{k/D}.x} \tag{8}$$

and the solution for x<0

$$c(x) = c_h.e^{\sqrt{k/D}.x} \tag{9}$$

The distance of a heterocyst from the minimum point follows then from (8)

$$x_s = \frac{1}{\sqrt{k/D}} \ln \frac{c_h}{c_o} \tag{10}$$

Thus there is a logarithmic relationship of the distance between the place of minimum concentration and the source on one hand, and c_h/c_o on the other hand.

Equation (10) is important because it enables us to determine the initial parameters in simulations of growing filaments.

If the concentration at the minimum equals the threshold concentration, so that $c_0=c_t$, then the distance $x_s=x'$ where x' is the critical distance associated with the induction of the next heterocyst.

Let us assume that the filament is growing exponentially everywhere at the same rate. This kind of growth can be characterized by letting the differential equation

$$\frac{dx}{dt} = rx \tag{11}$$

apply to the entire length of the filament.

The movement of a point on the filament as function of time is then

$$x(t) = x(Q)\ e^{rt} \tag{12}$$

If diffusion takes place faster than the expansion of the filament, an assumption which we discuss below, then steady state concentration can be reached in the filament while it is growing in length.

If x' is the distance between two adjacent heterocysts at the time when one of the heterocysts has just been formed, then when at a later time t' a new heterocyst arises between these two, its distance to each of the previous ones will again be x'. Thus a new heterocyst arises when the distance between two existing heterocysts doubles. This can be incorporated in the formula by stating that

$$2x' = x' . e^{rt'}$$

It follows that

$$t' = \frac{\ln 2}{r}$$

We see that t' is actually the doubling time for filament length, and it is in our model identical to the average length of time necessary for a cell to double (t_d or cell cycle time) for which it also holds that

$$t_d = \frac{\ln 2}{r} \qquad (13)$$

The average distance x' between heterocysts is obtained from equation (10) by substituting in it the threshold concentration c_t.

$$x_t = \frac{1}{\sqrt{k/D}} \ln \frac{c_h}{c_t} \qquad (14)$$

and observing that $x' = 2x_t$.

We see that in (14) the distance x_t is independent of the cell cycle time under the condition that diffusion is faster than expansion. Furthermore x_t is a function of two parameters only: $\sqrt{k/D}$ and c_h/c_t.

We can give an estimate of the lower boundary for the cell cycle time t_d above which steady state conditions prevail (see the last section). This estimate comes from the expression

for reaching a certain concentration c in the case of one-dimensional diffusion and decay in a semi-infinite medium with a single source (Crank, 1970, p.130):

$$\frac{c_x}{c_h} = \tfrac{1}{2} \exp(-x\sqrt{k/D})\ \mathrm{erfc}\left(\frac{x}{2\sqrt{Dt}} - \sqrt{kt}\right) +$$

$$+ \tfrac{1}{2} \exp(x\sqrt{k/D})\ \mathrm{erfc}\left(\frac{x}{2\sqrt{Dt}} + \sqrt{kt}\right) \qquad (15)$$

The limit for $t \to \infty$ of equation (15) is our previous expression (9).

From (15) we can calculate the time necessary to reach 99% of the equilibrium concentration everywhere in a semi-infinite medium and verify this calculation with simulation experiments. Such a calculation is similar to the one presented by Crick (1970) in which the time is estimated which is needed to come within 1% of equilibrium concentrations in source-sink diffusion systems without decay for embryonic gradient mechanisms. His formula is derivable from the following equation of Crank (1970, p.19).

$$\frac{c_x}{c_h} = \mathrm{erfc}\ \frac{x}{2\sqrt{Dt}}$$

which holds for diffusion in semi-infinite medium with source kept at constant concentration and the initial concentration being zero throughout the medium.

3. DISCRETE MODEL

In a cellular filament we are dealing with two transport processes: the transport in the cell itself, and the diffusion through the cell walls and membranes. The concentration gradients are therefore primarily present over the cell walls and membranes.

We discretize the previous continuous diffusion-decay model in the following way. Let us consider 3 neighbouring cells with concentration c_{x-1}, c_x and c_{x+1}. Here x is an integer variable standing for the number of cell lengths.

The concentration gradients between them are (if the length of each cell is equal to Δl):

$$g_{(x-1,x)} = \frac{c_{x-1} - c_x}{\Delta l} \quad , \quad g_{(x,x+1)} = \frac{c_x - c_{x+1}}{\Delta l}$$

The derivative of the gradient at cell x is then

$$\frac{\partial g_x}{\partial x} = \frac{g_{(x-1,x)} - g_{(x,x+1)}}{\Delta l}$$

By discretizing the modified Fick's equation we obtain the difference equation:

$$\Delta c_x = D \cdot \frac{\Delta t}{(\Delta l)^2} (c_{x-1} - c_x - c_x + c_{x+1}) - k.c_x \Delta t \qquad (16)$$

In our simulation obviously $\Delta l = 1$ and $\Delta t = 1$. When we wish to compare the simulation parameters with physical ones, then physical values have to be found for Δl and Δt. Thus the simulation values for diffusion and decay constants are: $D = D^* \frac{t}{(\Delta l)^2}$ and $k = k^* \Delta t$, and the physical values of these constants are D^* and k^*.

In the case of steady state, c_x does not change in time, thus $\Delta c_x = 0$, and

$$D c_{x-1} - 2Dc_x + Dc_{x+1} - kc_x = 0 \qquad (17)$$

For each term c_y a solution exists of the form λ^y. Then by substitution in (17) we obtain

$$D \lambda^{x-1} - 2D\lambda^x + D\lambda^{x+1} - k\lambda^x = 0 \qquad (18)$$

This yields

$$\lambda^{x-1} (D - (2D+k) \lambda + D\lambda^2) = 0$$

which is satisfied only if

$$D-(2D+k)\lambda + D\lambda^2 = \lambda^2 - (2+k/D)\lambda + 1 = 0. \qquad (19)$$

This quadratic equation has two roots:

$$\lambda_{1,2} = \frac{(2+k/D) \pm \sqrt{(2+k/D)^2 - 4}}{2} = 1 + \frac{k}{2D} \pm \sqrt{k/D + (\frac{k}{2D})^2} \quad (20)$$

Since the first and third coefficients of this quadratic equation are equal, we know that $\lambda_1 = \frac{1}{\lambda_2}$.

The general solution for c_x in equilibrium is

$$c_x = p.\lambda_1^x + Q.\lambda_2^x = p\,\lambda_1^x + Q\,\lambda_1^{-x} \quad (21)$$

In our problem we have two identical constant sources of the inhibitor. Thus the solution has to be a symmetric function with respect to the center point between the sources. Let us choose our coordinate system for x with origin at the center point.

If the distance of the sources are $\underline{a}$ and $\underline{-a}$ from the origin, then

$$c_a = c_{-a}$$

and

$$p\lambda_1^a + Q\lambda_1^{-a} - p\lambda_1^{-a} - Q\lambda_1^a = 0.$$

Thus

$$(P-Q)\,(\lambda_1^a - \lambda_1^{-a}) = 0.$$

This can only be true if P=Q.

Our solution is then

$$c_x = p\,(\lambda_1^x + \lambda_1^{-x}) \quad (22)$$

If the concentration at x=0 is c_1, then since $\lambda_1^0=1$ we obtain $P=c_0/2$, and therefore

$$c_x = \tfrac{1}{2}\,c_0\,(\lambda_1^x + \lambda_1^{-x}) \quad (23)$$

This equation is analogous to (7) for the continuous case, and

like in that case one of the two terms becomes dominant for $x>0$ or $x<0$.

We can also calculate the distance x_t from a source (heterocyst) where the threshold value c_t is found (for $x>0$).

$$c_t = c_h \cdot \lambda_1^{-x_t}$$

From this we obtain

$$\ln (c_h/c_t) = x_t \cdot \ln \lambda_1$$

$$x_t = \frac{\ln (c_h/c_t)}{\ln \lambda_1} \qquad (24)$$

There is thus a logarithmic relationship between x_t and the parameter c_h/c_t.

If we compare the discrete result (24) with that of the continuous model (equation 14) we see that the value of the coefficient in the discrete case is $\frac{1}{\ln \lambda_1}$ and in the continuous case it is $\frac{1}{\sqrt{k/D}}$.
The relationship between the two coefficients can be better understood by observing that from (20)

$$\lambda_1 = 1 + \frac{k}{2D} + \sqrt{k/D + (\frac{k}{2D})^2}$$

and that by Taylor series expansion

$$e^{\sqrt{k/D}} = 1 + \sqrt{k/D} + \frac{k}{2D} + \frac{k/D.\sqrt{k/D}}{6} + \ldots$$

Thus the 3 largest terms in the series are present in the expression for λ_1, and thereby $\ln \lambda_1$ is an approximation of $\ln e^{\sqrt{k/D}} = \sqrt{k/D}$. This approximation is valid in the interval below a k/D ratio of 100, i.e. a $\sqrt{k/D}$ value of 10. When this value is exceeded then the discrete coefficient begins to rise above the continuous one. As an example, let us take the case of D=k. Note that the assumption that the simulation value K

and D are equal does not imply that their physical values are equal (see last section). Then from equation (19) we can derive the characteristic equation

$$\lambda^2 - 3\lambda + 1 = 0$$

which has the roots

$$\lambda_1 = \frac{3 + \sqrt{5}}{2} \quad \text{and} \quad \lambda_2 = \frac{3 - \sqrt{5}}{2}$$

Thus for x_t we obtain the function

$$x_t = \frac{1}{\ln(\frac{3+\sqrt{5}}{2})} \cdot \ln(c_h/c_t)$$

and the value of its coefficient is

$$\ln \frac{1}{(\frac{3+\sqrt{5}}{2})} = 1.039043.$$

This value is thus 4% higher than that of the coefficient of the continuous equation

$$\frac{1}{\sqrt{k/D}} = 1.$$

4. SIMULATION METHODS AND RESULTS

We have carried out simulation experiments based on the above discrete model. The parameters of these simulations are: c_h/c_t, k/D and t_d the average cell cycle length. The last of these parameters represents the mean value of the number of simulation steps which are needed for a vegetative cell to undergo a complete cell cycle (from division to division). This was programmed by adopting a certain value for the mean length of cell cycle, and by allowing random variation around this value within a spread of ± 10% (This variability is not a Gaussian distribution since all values within the allowed spread are equally probable to occur).

The simulations were carried out with the help of the program CELIA (an acronym for "cellular linear array

simulator") which was originally written by Baker & Herman (1972) and variously extended and modified in Buffalo by Herman & Liu (1973) and in Utrecht by Frijters (1976). This program (written in FORTRAN) simulates the growth of cellular filaments in the sense that it allows the insertion or deletion of new cells in an existing filament. Each cell can be present in various states with respect to a number of attributes. The states can be expressed either as integer or as real numbers. Transition rules must be provided for each possible combination of attribute values and CELIA applies these rules in a parallel way to all cells in the filament. Thus changes of cellular states occur synchronously at discrete time steps. The state of a cell at the next time step is determined by its present state (with respect to all its attributes), and the states of k neighbour cells to the left and 1 neighbour cells to the right. The main program of CELIA keeps a double administration: the administration of the old string and the administration of the string which is being processed. There are subprograms for the calculations of the new values of various attributes.

For our simulation we defined the following attributes:

cell type: "V" for vegetative cells and "H" for heterocyst

inhibitor concentration: between 0 and 922.5

cell cycle length: mean between 0 and 132, spread + 10%.

The new inhibitor concentration c_x' of a given cell is calculated on the basis of equation (16), with the provision that D=k:

$$c_x' = c_x + \Delta c_x = D\,(c_{x-1} + c_{x+1} - 3c_x) + c_x \qquad (25)$$

A vegetative cell becomes a heterocyst when its concentration is equal to or less than the threshold concentration c_t. Each heterocyst has a constant concentration c_h.

A cell divides when its cell cycle attribute equals 0. In each time step this attribute is diminished by one in all vegetative cells. The sister cells resulting from a division receive cell cycle values assigned to them by a random number generator within the allowed spread around the mean value.

The initial concentrations of the filament are obtained from an equilibrium calculation for a string of 9 cells between two heterocysts. The cell cycle values of these cells are assigned at random. The end cells of the filament have neighbours with 0 concentration. Computations are usually carried out for 300 time steps.

A sample calculation sequence is shown in Table 1. The following values are used for this simulation:

$c_h = 922.5, \quad c_t = 0{,}48, \quad D = 0.25, \quad k = 0.25,$

mean cycle length = 80.

There are 6 cell divisions taking place and one new heterocyst is formed in this sequence. The average distance between heterocysts in the whole simulation (300 steps) is 11.0.

Before we discuss our computations concerning the estimation of the parameters of these models, we want to consider the observed heterocyst distances and their relationship to the predicted x_t values. Let us designate the observed average heterocyst distance as d. In fact, we have observed in the simulations the ratio of total cell number to number of heterocysts and take this ratio as the average distance between two heterocysts.

We assume that the number of vegetative cells increases exponentially in the filament. The distance between two heterocysts at the moment when one of them is just formed is x_t. The distance between the heterocysts then increases until it becomes $2x_t$, at which time a new heterocyst will arise. The mean distance during this time is given by the following formula

$$d = \frac{1}{t_d} \int_0^{t_d} x_t \, e^{rt} \, dt \qquad (26)$$

where t_d is the doubling time or cell cycle length and $r = \frac{\ln 2}{t_d}$. The solution of this integral is

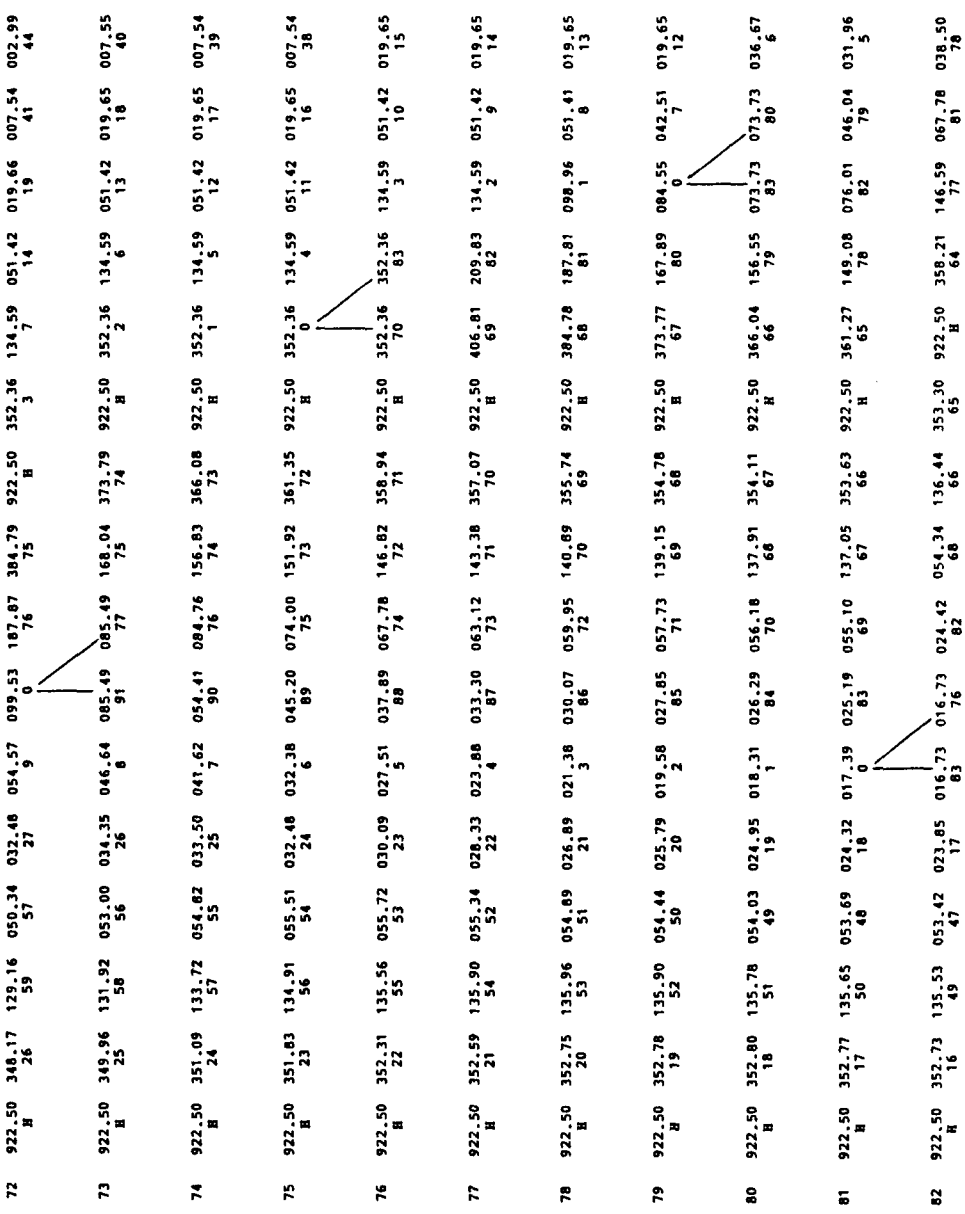

number of steps until division), except for the heterocysts which are designated as "H". Lines indicate the daughter cells resulting from a cell division, and the arrow shows the transformation of a vegetative cell into a heterocyst as a result of the concentration falling below the threshold value.

72	001.33 70	000.82 85	000.81 4	001.35 24	003.04 31	007.64 75	019.74 77	051.49 34	134.64 15	352.39 1	922.50 H						
73	002.96 43	001.28 69	000.74 84	000.75 3	001.30 23	003.01 30	007.60 74	019.72 76	051.47 33	134.63 14	352.38 0	922.50 H					
74	002.95 42	001.25 68	000.69 83	000.70 2	001.26 22	002.98 29	007.58 73	019.70 75	051.45 32	134.62 13	352.38 73	352.38 73	922.50 H				
75	002.93 41	001.22 67	000.66 82	000.66 1	001.24 21	002.96 28	007.56 72	019.68 74	051.44 31	134.61 12	209.84 72	406.81 72	922.50 H				
76	007.53 37	002.92 40	001.20 66	000.64 81	000.64 0	001.21 20	002.94 27	007.55 71	019.67 73	051.44 30	098.98 11	187.82 71	384.79 71	922.50 H			
77	007.53 36	002.91 39	001.19 65	000.62 80	000.62 70	000.62 92	001.20 19	002.93 26	007.54 70	019.66 72	042.52 29	084.56 10	167.90 70	373.78 70	922.50 H		
78	007.52 35	002.91 38	001.18 64	000.61 79	000.47 69	000.61 91	001.19 18	002.92 25	007.53 69	017.43 71	036.69 28	073.74 9	156.56 69	366.04 69	922.50 H		
79	007.52 34	002.90 37	001.17 63	000.56 78	922.50 H	000.57 90	001.18 17	002.91 24	006.97 68	015.41 70	031.97 27	066.75 8	149.09 68	361.28 68	922.50 H		
80	017.42 11	007.52 33	002.90 36	001.16 62	231.06 77	922.50 H	231.06 89	001.16 16	002.76 23	006.32 67	013.59 69	028.53 26	061.95 7	144.28 67	358.22 67	922.50 H	
81	015.40 10	006.96 32	002.89 35	058.78 61	288.68 76	922.50 H	288.68 88	058.75 15	002.56 22	005.67 66	012.11 68	026.02 25	058.69 6	141.11 66	356.25 66	922.50 H	
82	023.35 4	013.58 9	006.31 31	017.16 34	087.59 60	317.49 75	922.50 H	317.48 87	087.50 14	016.74 21	005.09 65	010.95 67	024.20 24	056.45 5	139.01 65	354.96 65	922.50 H

Table 1. Ten iteration steps from a simulation run with the program CELIA. The parameter values are: $c_h = 922.5$, $c_t = 0.48$, $D = k = 0.25$, cell cycle length $t_d = 80 \pm 10\%$. Each cell is represented by two numbers, the upper number showing the inhibitor concentration and the lower number the cell age (the remaining

$$d = \left[\frac{1}{t_d} \cdot \frac{x_t}{r} e^{rt}\right]_0^{t_d} = \frac{1}{t_d}\left(\frac{x_t}{r} \cdot e^{rt_d} - \frac{x_t}{r}\right) = \frac{x_t}{rt_d}\left(e^{rt_d} - 1\right)$$

Since

$$r = \frac{\ln 2}{t_d}, \quad d = \frac{x_t}{\ln 2}\left(e^{\ln 2} - 1\right) = \frac{x_t}{\ln 2} \tag{27}$$

On the basis of formula (27) we can calculate the expected average distances between heterocysts for various values of c_h/c_t, and compare these distances with those found in simulations. In Table 2 we show a number of such comparisons.

There is a reasonable good agreement between the expected and simulated heterocyst distances.

c_t	$\ln \frac{c_h}{c_t}$	expected d (discrete model)	expected d (continuous model)	value of d from simulation
0.02	10.33	15.5	14.9	14.9
0.04	9.64	14.4	13.9	12.9
0.08	8.95	13.4	12.9	12.7
0.16	8.25	12.3	11.9	10.7
0.32	7.56	11.3	10.9	11.1
0.64	6.87	10.3	9.9	9.9
1.28	6.17	9.2	8.9	6.8
2.56	5.48	8.2	7.9	8.2
5.12	4.79	7.1	6.9	7.1
10.24	4.10	6.1	5.9	5.3
20.48	3.40	5.1	4.9	3.3
40.96	2.71	4.0	3.9	2.5

Table 2. Expected and observed values of average heterocyst distance for different threshold concentrations. In all cases $c_h = 615$, $D = k = 0.25$ and $t_d = 120$.

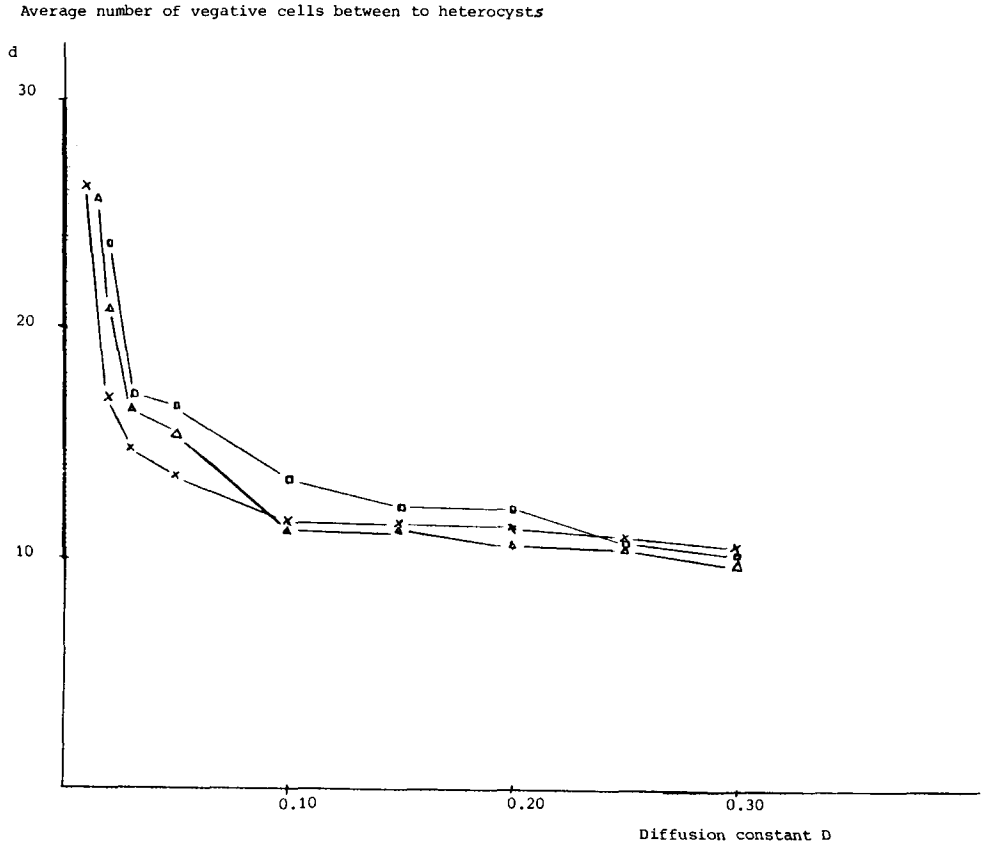

Figure 3. Average number of vegetative cells between two heterocysts (d) as function of the simulation value of the diffusion constant (D). Curves are obtained from simulation runs with parameters $\ln(c_h/c_t) = 6.89$, $k = D$, and the cell cycle length varied as follows: x ... 120 ± 10%, Δ... 90 ± 10%, □ ... 60 ± 10%.

In the simulation shown in Table 1 the c_h/c_t ratio of 922.5/0.48 is the same as the ratio 615/0.32 used in one of the rows of Table 2. The heterocyst distance in both cases is about 11, which agrees well with the expected values.

We should point out that the observation of the average heterocyst distance in real organisms is not sufficient to give us an estimate of the parameters c_h/c_t and k/D since both of them are affecting the value of x_t and thereby of $\underline{d}$. However, the development of regular heterocyst patterns (without multiple heterocyst appearing) depends on the D and k parameter values in conjunction with cell cycle times. From simulation experiments in which D and k are varied, one can find domains of regular patterns for these parameters independently from the value of c_h/c_t but dependent on t_d. An example is shown in Figure 3, where the effect of the variation of D and k as well as of t_d is shown on the average number of vegetative cells between heterocysts (with a constant ln (c_h/c_t) = 6.89 value).

We see that for t_d = 120 the domain of normal behaviour (about 10 cells between heterocysts) is present for D = k values above 0.12, for t_d = 90 it is above D = k = 0.11, and for t_d = 60 it is above D = k = 0.15. These limit values can serve to give independent estimates for D and k in the model. Note that D cannot be greater than 0.33 because above this value instability arises due to the fact that more inhibitor can leave a cell than the amount that enters.

The growth rate of a filament (the change in cell number) is determined primarily by the cell doubling time t_d and secondarily by the other two parameters, since the cells which turn into heterocysts do not divide anymore.

The growth function is an exponential function corresponding to the differential equations

$$\frac{dV}{dt} = (r-\alpha)\ V$$

$$\frac{dH}{dt} = \alpha V$$

where V(t) and H(t) are the numbers of vegetative cells and heterocysts at time t, α is the rate of which vegetative cells are transformed into heterocysts, and r is the rate of multiplication of vegetative cells. We have seen that $r = \frac{\ln 2}{t_d}$ (formula 13), but we have no corresponding explicit formula for α as function of the other parameters.

5. CONCLUSIONS

We can also attempt to correlate our simulation parameters with physical parameters observed in the filaments.

According to measurements by Wilcox et al. (1973), the average time between successive divisions of vegetative cells growing at 24° on solid media is 14-15 hrs for *Anabaena catenula*, and 23-28 hrs for *A. cylindrica*. The number of vegetative cells between nearest heterocysts or proheterocysts in young filaments has a mean of 10.1 ± 2.5 cells in the first organism and a mean of 9.3 ± 2.8 cells in the second organism. Finally, the average length of vegetative cells in these organisms is 7.2 μm and 5.5 μm, respectively.

Since in the simulations for Table 2 we have adopted the value of 120 iteration steps per division, we can easily find that for *A. catenula* one iteration step would correspond to 7.0-7.5 minutes, while for *A. cylindrica* one iteration step would be 11.5-14.0 minutes.

In order to find a physical value for the critical inhibition distance x_t between two heterocysts (the distance at which the threshold concentration is reached at equilibrium), we should recall that

$$x_t = \ln 2 \cdot d$$

where d is the average observed distance between heterocysts. From the above data we obtain the physical value of $x_t = 10.1 \times 7.2 \times \ln 2 = 50.4$ μm for *A. catenula*, and a value of $x_t = 9.3 \times 5.5 \times \ln 2 = 35.5$ μm for *A. cylindrica*. The value of about 50 μm in the case of *A. catenula* agrees well

with the minimum distance seen in the microphotographs of Mitchison & Wilcox (1972) (Fig. 1).

For *A. catenula* we have therefore the following physical values:

$\Delta t = 7.25$ min $= 435$ sec

$\Delta l = 7.2$ m $= 7.2 \times 10^{-6}$ m

We have seen previously that the physical constants for diffusion and decay are:

$$D^* = D \frac{(\Delta l)^2}{\Delta t} \quad \text{and} \quad k^* = \frac{k}{\Delta t}$$

In our considerations on feasible simulation values for D and k we came to the estimate that for a regular heterocyst pattern

$0.12 < D < 0.33.$, and $t_D > 60.$

In terms of physical units, this means that

$t_D^* > 60 \times 7.25$ min $= 7.25$ hrs and

1.43×10^{-14} m^2/sec $< D^* < 3.93 \times 10^{-14}$ m^2/sec

Thus the actual diffusion constant in the filaments must have a value of between 1.4 and 3.9×10^{-14} m^2/sec, which is a rather low value for diffusion in water at room temperature. An organic molecule of molecular weight 100 to 200 (such as glutamine) has a diffusion constant in water at 20° of about 10×10^{-10} m^2/sec. But in the case of cellular filaments we have to take into account an average diffusion velocity in cells and in cell membranes, for which the above estimated value is not unreasonable.

In our simulations we have assumed that k = D. This refers to the simulation values of these constants and obviously does not imply that their physical values are identical. This would yield the following estimate for the physical value of the decay constant:

2.7×10^{-4} sec$^{-1} < k^* < 7.5 \times 10^{-4}$ sec^{-1}

These are reasonable values for a reaction constant concerning enzymatic breakdown of the inhibitor.

As far as the cell cycle length of 7.25 hrs is concerned, this value is well below the 24 hr length observed in rapidly growing *Anabaena* cultures (Wilcox et al., 1973). The bounds for the physical values D^*, k^* and t_D^* of the diffusion, decay and cell cycle constants represent the main biological predictions of this model.

Wolk et al. (1974) obtained an estimation of the physical values of k and D by following the movement of ^{13}N-labelled compounds in the filaments. Their conclusion concerning the D value is probably incorrect because it is based on the movement of all N-containing compounds between the cells. Their value for D^* appears to be above the value 5×10^{-12} m^2/sec (recalculated from their estimate of $\tau < 5$ sec. $cell^{-2}$). The value they obtained for the decay constant k^* is probably valid and is estimated at 8×10^{-4} sec^{-1}. This is in excellent agreement with our estimate above.

The above estimate of the diffusion constant for a morphogenetic inhibitor in blue-green bacteria is surprisingly close to that found in a model for phyllotaxis (leaf primordium determination on the apex of higher plants) by Veen & Lindenmayer (1977). There the estimates were

$$D^* \tilde{=} 0.4 \times 10^{-14} \; m^2/sec$$

and

$$k^* < 2 \times 10^{-4} \; sec^{-1}.$$

That diffusion processes involved in morphogenesis have similar physical parameters in widely different organisms was assumed by Crick (1970) already.

Our choice of the simulation values $k = D$ in the present paper made the model simpler by reducing the number of parameters and was based originally on the idea that decay can be considered an analogue of diffusion out of the cells. Since the dimensions of these constants are not the same, the physical values of the diffusion and decay constants are obviously not identical. But further investigation is clearly

necessary on extending the model to independently chosen values of k and D.

Another way in which the model could be made more realistic, but also more complex, is by introducing a gradual increase in the inhibitor concentration in a recently initiated heterocyst. This would take into account the fact that newly formed heterocysts cannot immediately fix nitrogen. Thus the value of c_h should increase as a function of time.

The theoretical methods by which we arrived at estimates of the physico-chemical parameters can contribute to experimental tests of the hypotheses incorporated into our model. Particularly the nature and mode of transport of the nitrogen-rich inhibitor needs to be further investigated in the light of the predictions provided by the model. Another interesting aspect of morphogenesis in blue-green bacteria for future investigations is the suppression of branching habit in *Anabaena doliolum* by added nitrogen in the medium (Dhar, 1979). Other studies have suggested that the branching character is governed by a single or at most a few genes. This indicates that the induction mechanism may be related to that of heterocyst induction. The practical uses of nitrogen-fixing cyanobacteria have been reviewed in Hall et al., 1985).

REFERENCES

1. Baker, R.W. and Herman, G.T. (1972). Simulation of organisms using a developmental model I. Basic description. II. The heterocyst formation problem in blue-green algae.- Bio-Med. Computing 3: 201-215, 251-267.
2. Bothe, H., Nelles, H., Kentemick, T., Papen, H. and Neuer, G. (1984). Recent aspects of heterocyst biochemistry and differentiation. In W. Wiessner, D. Robinson, R.C. Starr, eds., Compartments in Algal Cells and Their Interaction, 218-232.- Berlin, Springer Verlag.
3. Crank, J. (1970). The Mathematics of Diffusion.- Oxford, Oxford Univ. Press.
4. Crick, F. (1970). Diffusion in embryogenesis.- Nature 225: 420-422.
5. Dhar, B. (1979). Nutritional control of the frequency of MNNG-induced true branching habit in *Anabaena doliolum*.- Molec. Gen. Genetics 173: 177-181.
6. Fogg, G.E. (1949). Growth and heterocyst production in *Anabaena cylindrica* in relation to carbon and nitrogen metabolism.- Ann. Bot. 13: 241-159.

7. Frijters, D. (1976). An automata-theoretical model of the vegetative and flowering development of *Hieracium murorum* L.- Biol. Cybern. 24: 1-13.
8. Golden, J.W., Robinson, S.J. and Haselkorn, R. (1985). Rearrangement of nitrogen fixation genes during heterocyst differentiation in the cyanobacterium *Anabaena*.- Nature 314: 419-423.
9. Hall, D.O., Affolter, D.A., Brouers, M., Shi, D.-J., Yang, L.-W. and Rao, K.K. (1985). Photobiological production of fuels and chemicals by immobilized algae.- Ann. Proc. Phytochem. Soc. Eur. 26: 161-185.
10. Herman, G.T. and Liu, W.H. (1973). The daughter of CELIA, the French flag and the firing squad.- Simulation 21: 33-41.
11. Mitchison, G.J. and Wilcox, M. (1972). A rule governing cell division in *Anabaena*.- Nature 239: 110-111.
12. Mitchison, G.J., Wilcox, M. and Smith, R.J. (1976). Measurement of an inhibitory zone.- Science 191: 866-867.
13. Reddy, P.M. and Talpasayi, E.R.S. (1974). Heterocyst formation in the blue-green alga, *Cylindrospermum*.- Nature 249: 493-494.
14. Singh, H.N. (1973). Influence of nitrogen nutrition on spontaneous mutation in the blue-green alga *Anabaena doliolum*.- Mutation Research 18: 233-235.
15. Streicher, S.L., Shanmugam, K.T., Ausubel, F., Morandi, C. and Goldberg, R.B. (1974). Regulation of nitrogen fixation in *Klebsiella pneumoniae:* evidence for a role of glutamine synthetase as a regulator of nitrogenase synthesis.- J. Bact. 120: 815-821.
16. Thomas, J., Meeks, J.C., Wolk, C.P., Shaffer, P.W., Austin, S.M., and Chien, W.S. (1977). Formation of glutamine from (^{13}N) ammonia, (^{13}N) dinitrogen, and (^{14}C) glutamate by heterocysts isolated from *Anabaena cylindrica*.- J. Bact. 129: 1545-1555.
17. Veen, A.H. and Lindenmayer, A. (1977). Diffusion mechanism for phyotaxis.- Plant Physiol. 60: 127-139.
18. Wilcox, M., Mitchison, G.J. and Smith, R.J. (1973). Pattern formation in the blue-green algae, *Anabaena*. I. Basic mechanisms. II. Controlled proheterocyst regression.- J. Cell Science 12: 707-723, 13: 637-649.
19. Wolk, C.P. (1967). Physiological basis of the pattern of vegetative growth of a blue-green algae.- Proc. Nat. Acad. Sci. U.S.A. 57: 1246-1251.
20. Wolk, C.P. and Quine, M.P. (1975). Formation of one-dimensional patterns by stochastic processes and by filamentous blue-green algae.- Dev. Biol. 46: 370-382.
21. Wolk, C.P., Austin, S.M., Borthis, J. and Galonsky, A. (1974). Autoradiographic localization of ^{13}N after fixation of ^{13}N-labeled nitrogen gas by a heterocyst -forming blue-green algae.- J. Cell Biol. 61: 440-453.
22. Wolk, C.P., Thomas, J., Shaffer, P.W., Austin, S.M. and Chien, W.S. (1976). Pathway of nitrogen metabolism after fixation of ^{13}N-labeled nitrogen gas by the cyanobacterium, *Anabaena cylindrica*.- J. Biol. Chem. 251: 5027-5034.